Journal of Engineering and Applied Sciences 11 (5): 1044-1057, 2016
ISSN: 1816-949X

Three Phase Four Wires PMSG Energy Source Generation with Maximum Point Tracking

[1]Djamel Derardja, [2]Wassila Issaadi, [2]Abdelkrim Khireddine and [3]Abdelhamid Hamadi
[1]Maritime Sciences Electrical Engineering Laboratory,
Ecole Nationale Superieure Maritime, ENSM Bou-Ismail, Algeria
[2]Faculty of Technology, Electrical Engineering Laboratory,
Algeria Superior Technology School, University of Bejaia, 06000 Bejaia, Montreal, Canada

Abstract: This study deals with design and control of a connected wind energy generation system employing a Permanent Synchronous Generator (PMSG) is driven by a variable speed wind turbine for three-phase four-wire local loads. The proposed energy conversion system uses back to back connected Pulse Width Modulated (PWM) Insulated Gate Bipolar Transistors (IGBTs) based Voltage Source Converters (VSCs). The ac terminals of one VSC (stator side converter) are connected to the stator terminals of PMSG for the Maximum Power Tracking (MPT) through its rotor speed control. The grid side converter uses Adaline neural network for harmonics, reactive power and unbalanced compensation. The proposed system is modeled and simulated on MATLAB using simulink and Sim Power Systems (SPS) set toolboxes. The performance of the proposed system is presented to demonstrate its capability of MPT, harmonic elimination, load balancing and load leveling.

Key words: PMSG generator, MPPT, fuzzy logic, true MPPT, SPS, PWM

INTRODUCTION

To achieve fast dynamic response, the PMSG side converter is controlled by nonlinear control by decoupling the active (q-) and reactive (d-) components of stator currents. In the variable speed wind turbine, the speed of the generator is varied to achieve maximum coefficient of performance for the turbine as shown in Fig. 1 with rotor speed control of the PMSG. The grid side converter is controlled using neural network control for compensation of harmonics, reactive power, neutral current and unbalanced load (Maheshappa *et al*., 1998; Chiang *et al*., 1998; Muljadi, 1997; Taha and Suresh, 1996; Bose *et al*., 1985).

Adaline control technique of a grid-side inverter: The Adaline technique adjusts the weight to generate references and to reduce the error between the sensed signal and its references. These weights are variable and change as per the load current magnitude. The weights are updated using the LMS adoption algorithm tuned Adaline technique (Chim *et al*., 2011; Protin and Astier, 1997) as using RLS (least square mean) to reduce the error by updating the weights:

$$E = (d - y)^2 \tag{1}$$

With:

$$d = \text{target} = W_p(k)u_p(k)$$

$$y = \text{output} = \sum_{i=1}^{n} W_i \times X_i(t) \tag{2}$$

$$E = d^2 + y^2 - 2yd = d^2 + 2\times d\times \sum_{i=1}^{n} W_i \times X_i(t) - d\times\left(\sum_{i=1}^{n} W_i \times X_i(t)\right)^2 \tag{3}$$

$$\frac{\partial E}{\partial W_i} = -2\left[d - \sum_{i=1}^{n} W_i \times X_i(t)\right]X_i(t) \tag{4}$$

$$\begin{aligned} \Delta W_{ap}(k+1) &= \eta\left(i_{La}(k) - W_{ap}(k)u_{ap}(k)\right)u_{ap}(k) \\ \Delta W_{bp}(k+1) &= \eta\left(i_{Lb}(k) - W_{bp}(k)u_{bp}(k)\right)u_{bp}(k) \\ \Delta W_{cp}(k+1) &= \eta\left(i_{Lc}(k) - W_{cp}(k)u_{cp}(k)\right)u_{cp}(k) \end{aligned} \tag{5}$$

For a given learning rate, the local error will be reduced more rapidly by adjusting the weights according to the delta rule. Where, η is the coefficient of

Corresponding Author: Djamel Derardja, Maritime Sciences Electrical Engineering Laboratory,
Ecole Nationale Superieure Maritime, ENSM Bou-Ismail, Algeria

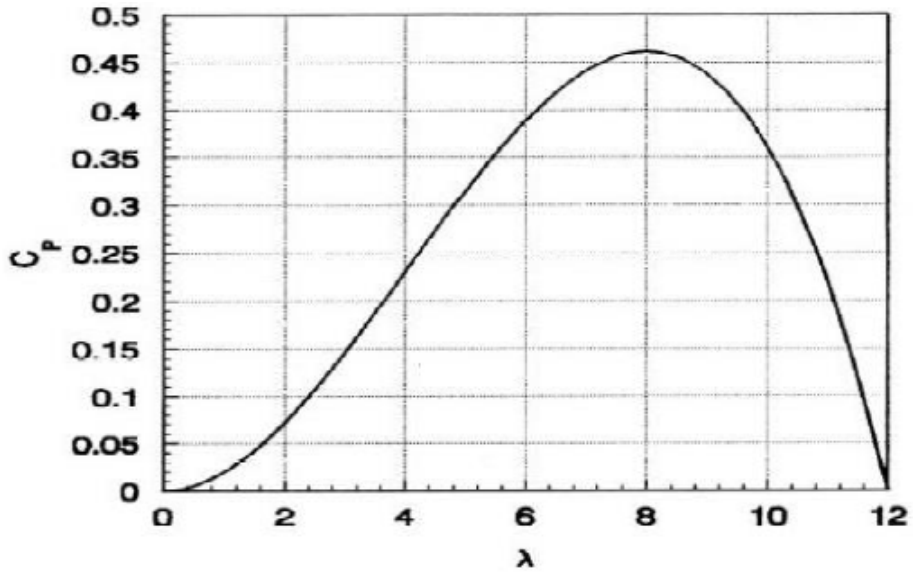

Fig. 1: Maximum coefficient of performance for the turbine

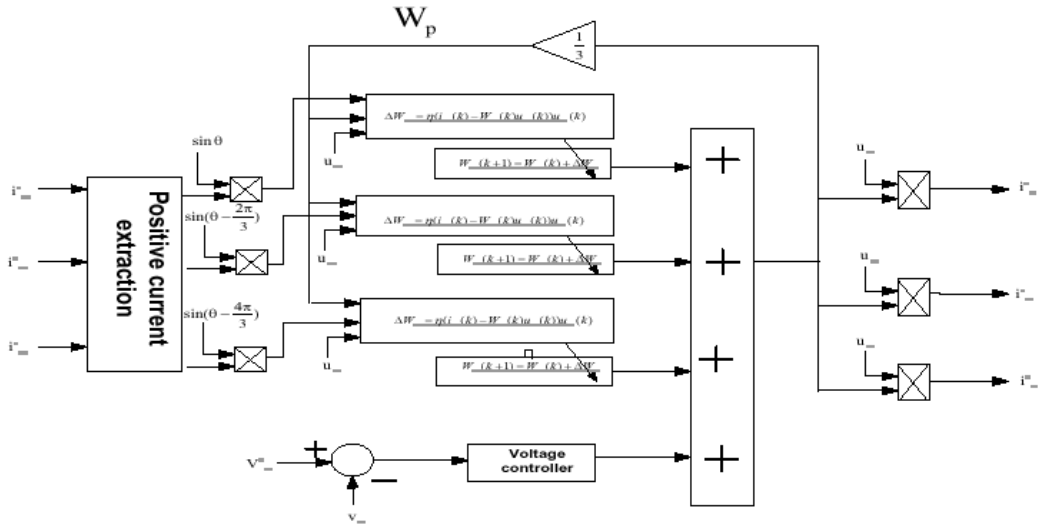

Fig. 2: Control scheme of inverter

convergence and k is the sampling instant. The value of η decides the rate of convergence and accuracy of estimation and the practical range of values lie in between 0.1 and 1.0. The average weight of the fundamental reference active-power component of the source current is given as:

$$W_p(k) = \frac{W_{loss}(k) + W_{ap}(k) + W_{bp}(k) + W_{cp}}{3} \quad (6)$$

The three-phase fundamental reference active-power component of the source currents are computed as follows:

$$\begin{aligned} i^*_{sap} &= W_p u_{ap} \\ i^*_{sbp} &= W_p u_{bp} \\ i^*_{scp} &= W_p u_{cp} \end{aligned} \quad (7)$$

Using a positive sequence of a current synchronized load with source voltage, there is no need to calculate the quadrature components of reference source currents (Fig. 2).

Control of permanent synchronous generator: The dynamic model of PMSG can be represented in dq reference frame (Dondi *et al*., 2008).

$$v_d = Ri_d - L_d\frac{di_d}{dt} + L_q\omega_r i_q$$
$$v_q = Ri_q - L_q\frac{di_d}{dt} + L_q\omega_r i_d + \omega_r\phi_m \quad (8)$$
$$J\frac{d\omega_r}{dt} = T_m + T - B\omega_r$$

Where:
T_e = Electromagnetic torque
T_m = Mechanical torque
J = Combined inertia moment of the WTG rotor and PMSG
ω_r = Rotor mechanical speed which is related to the rotor
P = Number of poles, ϕ_m .is magnetic flux
L_d = Direct axis inductance
L_q = Quadrature inductance
R = Resistance
ω_r = Rotor speed of generator
B = Coefficient of friction

The system is rearranged as:

$$\frac{di_d}{dt} = \frac{R}{L_d}i_d + \frac{L_q}{L_d}\omega_r i_q - \frac{V_d}{L_d}$$
$$\frac{di_q}{dt} = \frac{R}{L_q}i_q + \frac{L_d}{L_q}\omega_r i_d + \frac{\omega_r\phi_m}{L_q}\frac{V_q}{L_q} \quad (9)$$

Control formula:

$$V_d = -u_d - Ri_d + L_q\omega_r i_q =$$
$$V_q = -u_q - Ri_q - L_d\omega_r i_d + \omega_r\phi_m \quad (10)$$

Where:
u_d = New input in d axis
u_q = New input in q axis

Current reference generation:

$$i_d^* = 0$$

MATERIALS AND METHODS

Proposed MPPT and current reference in q axis for permanent synchronous generator: The MPPT Model (Khouzam, 1990) is obtained using the characteristics given in Fig. 3:

$$P_{mec} = \frac{1}{2}\rho AC_P(\lambda,\beta)V^3 \quad (11)$$

$$P_{mec} = \frac{1}{2}\rho AC_P(\lambda,\beta)V^3 =$$
$$v_{dc}i_{dc} \rightarrow i_{dc} = \frac{1}{2}\frac{\rho AC_P(\lambda,\beta)}{v_{dc}}V^3 \quad (12)$$

$$\Omega = \frac{V\lambda}{R} \quad (13)$$

$$i_{dc} = i_q = \frac{1}{2}\frac{\rho AC_P(\lambda,\beta)}{V_{dcr}}\left(\frac{R\Omega}{\lambda}\right)^3 \quad (14)$$

The reference speed is given by the choice of value of $\beta = 0$, $\lambda = \lambda_{nominal} = \lambda^*$ for $C_P = C_{Pmax}$. The speed reference is given by (Moller, 1993):

$$i_q^* = \frac{1}{2}\frac{\rho AC_{Pmax}(\lambda,\beta)}{V_{dcr}}\left(\frac{R\Omega^*}{\lambda^*}\right)^3 \quad (15)$$

The parameters C_{pmax} and $\lambda_{nominal}$ are determined using the model of the wind turbine given in Fig. 3.

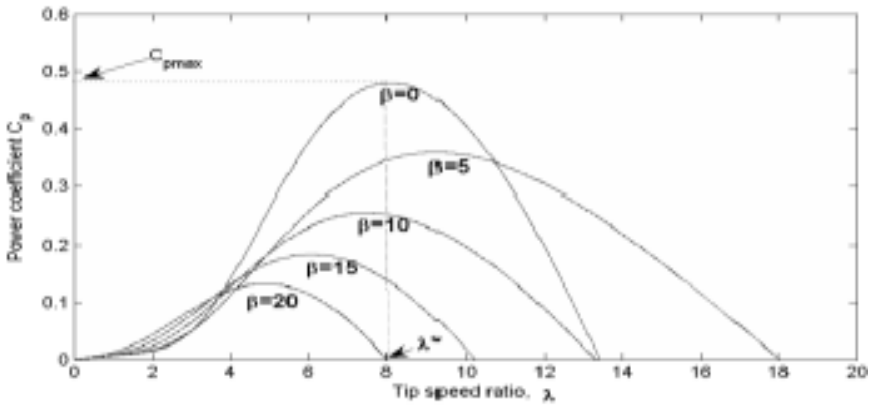

Fig. 3: Characteristics Cp versus λof the wind turbine

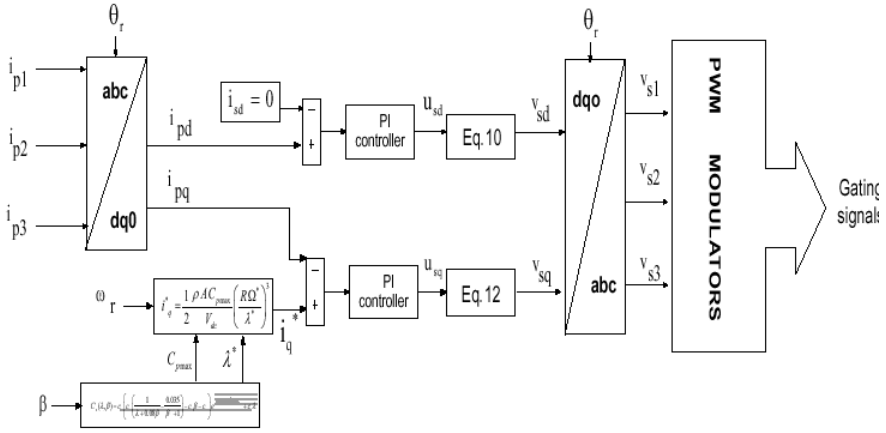

Fig. 4: Control scheme for rectifier

Table 1: Rated power of the wind turbine

Type of load	Maximum	Minimum	Mean
Nonlinear load	6 kW	3 kW	4.5 kW

Table 2: The rated power of wind turbine for maximum and mean powers

Variables	V = 6 m/s	V = 14 m/s
Maximum power	P_{pmsg} = 2 kW	P_{pmsg} = 7 kW
Mean power	P_{pmsg} = 3.5 kW	

Dondi *et al*., 2008; Khouzam, 1990; Moller, 1993; Tsuda *et al*., 1994; Campbell, 2007; Luque and Hegedus, 2003) the control scheme to control the boost converter is given in Fig. 4.

Design of wind-panel hybrid system: The proposed system is designed for the load varying between 3 and 6 kW. The average load of the system is considered to be 4.5kW. The rated power of wind turbine depends on the wind speed. For the design of the proposed system, the available wind turbine power is considered around 10 kW (Celik, 2003; DenHerder, 2006). For the wind system, a minimum and maximum wind speed is considered. Therefore, the rated power of the wind turbine is given in Table 1. As, we integrate the renewable energy sources and the utility grid with the net zero energy building to achieve NZEB. The rated power of wind turbine for maximum and mean powers is Table 2 the selection of voltage of DC link is given by:

$$V_{dc} \succ \frac{V_{LL\_grid}}{0.612 * m_a} = \frac{208}{0.612 * 1} = 339.86V \quad (16)$$

where, m_a is modulation index

PMSG design: For wind speeds the rated wind speed, the mechanical power P_m, captured by the wind turbine is a function of wind speed V, radius of turbine r, density of air r and coefficient of performance C_p and is given as follows:

$$P_m = \frac{1}{2} C_p A \rho V^3 \quad (17)$$

where, C_p is the ratio of speed of the tip of the turbine blade to wind speed as:

$$\lambda = \frac{\Omega_r R}{V} \quad (18)$$

where, Ω is the rotational speed of the PMSG. The relationship between coefficient of performance and tip speed ratio for a typical wind turbine is shown in Fig. 2. The maximum coefficient of performance (C_{pmax} = 0.46) is achieved at optimum tip ratio (λ = 8.1). Substituting, Pm = 10 kW, Cp = 0.46, wind speed V = 10 m sec^{-1} and density of air ρ = 1.25 kg/m^3, the radius of wind turbine R is obtained:

$$R = \sqrt{10000/\left(0.5 * 0.46 * 1.25 * \pi * (10)^3\right.} = 3.32 \text{ m} \quad (19)$$

Integration of renewable energy sources and the utility grid with the net zero energy building: The Net Zero Energy Building (NZEB) is an alternative to reduce the bill of electricity and to reduce the alarming pollution in the world. Thus the main objective is to integrate the Renewable Energy Sources (RES) and the utility grid with the electrical load of NZEB. The wind turbine parameters are:

- Number of blade = 3
- Wind speed range = 6-14 m sec^{-1}
- Radius of the blade = 3.32 m
- C_{pmax} = 0.46
- Λ* = 8.1

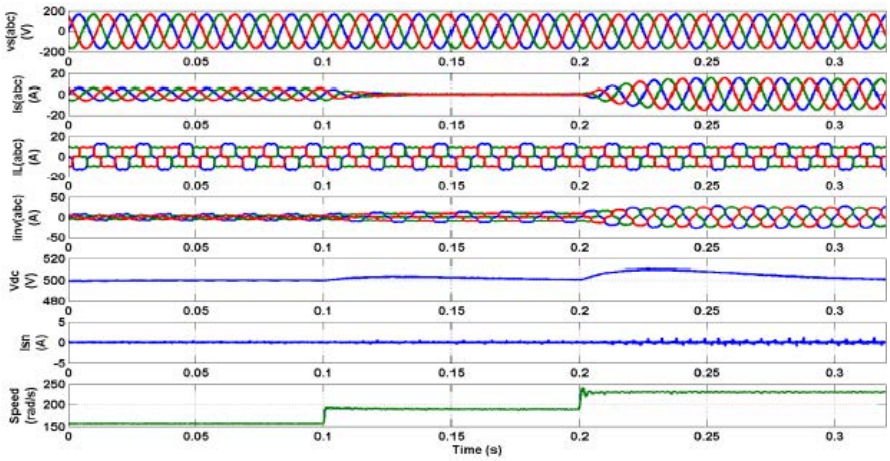

Fig. 5: Dynamic response of the system

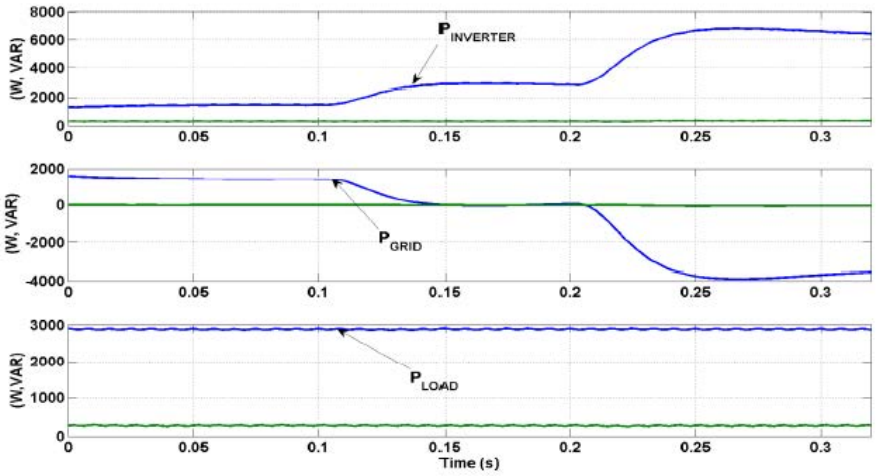

Fig. 6: Power flow analysis of the system

Table 3: PMSG data sheet

Stator voltage	Torque	Synchronous speed	Rated power	Stator resistance	Inductor	Pairs of poles
273 V	2.3/A NM	2500 rpm	10 kW	0.08 Ω	0.006 H	8

PMSG data sheet available given by: PMSG data sheet shown in Table 3. By using MATLAB simulink and SimPower Systems (SPS) set Toolboxes, simulations results are shown in Fig. 5 and 6.

RESULTS AND DISCUSSION

Simulations: Simulation is a powerful tool for assessing the theoretical performance of different systems. The test device can be functioned in easily controllable conditions and its execution can be precisely monitored. We established with SIMULINK physical subsets such as the solar panel, wind, load, the chopper and MPPT controller as independent units and to check their appropriate functionality. Finally, these subsets can be combined to form a complete hybrid power system with a PPM (Maximum Power Point) control (Wassila *et al.*, 2016). The values for cells Temperature (T), irradiation (R), the number of photovoltaic cells in series are available as external variables and can be changed at any time during the simulation process. This allows the observation and evaluation of the system response to sudden changes in operating conditions.

Photovoltaic generator: The photovoltaic generator is modeled by GPV following Eq. 20:

$$I = n_p\left[I_L - I_s\left(e^{q(v/vs+IRs/np)/AKT}-1\right)-\left(V/ns+IR_s/n_p\right)/R_p\right] \quad (20)$$

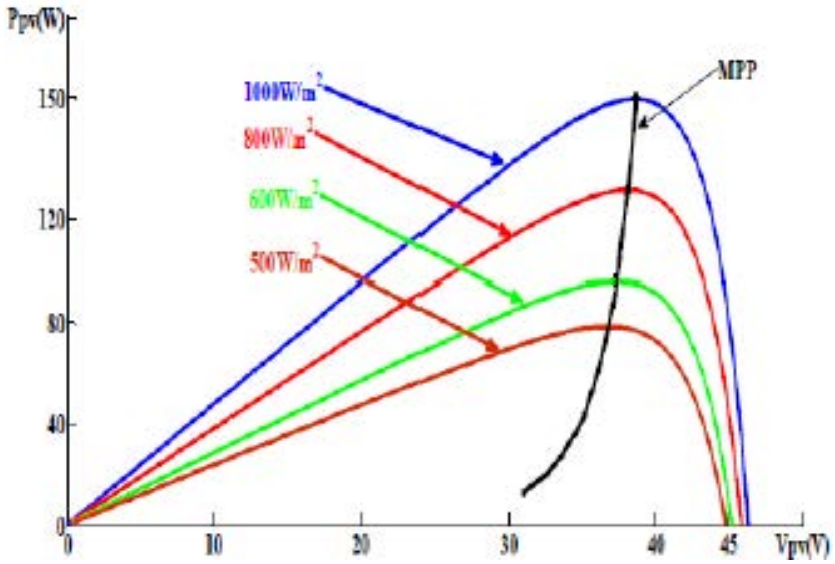

Fig. 7: Changing the MPP according to the brightness

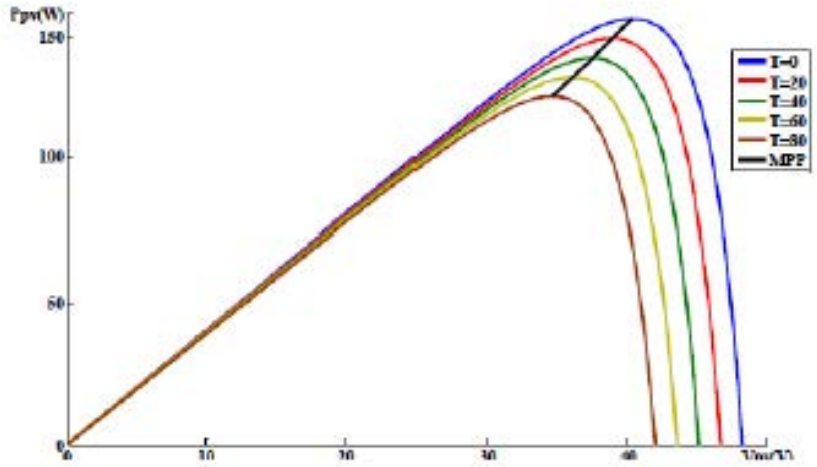

Fig. 8: Temperature influence on MMP

$$p = IV \tag{21}$$

$$I = n_p V\left[\begin{array}{l} IL - I_s\left(e^{q(v/vs+PRs/Vnp)/AKT} - 1\right) - \\ \left(V/ns + PR_{s/}Vn_p\right)/R_p \end{array}\right] \tag{22}$$

The current I of the solar panel is according the current IL current generated by photon irradiation solar is is the saturation current given by the manufacturer, ns and np are the number of respectively cells in series and in parallel, A is perfect junction factor PN. K is the Boltzmann coefficient = $1.38.10^{-23}$J/K. T is the temperature, the voltage across the panel solar is V. The power delivered by the panel P is expressed by Eq. 21. The GPV is heavily influenced by the variation of brightness and temperature. Indeed in Fig. 7 is the GPV subjected to changes in brightness where it appears clearly the reduction of the power and the change the maximum power point MPP).

In Fig. 8 the PV array GPV is subject to temperature variation in brightness constant, again the maximum power point MPP exchange. This entails reconciling these behaviors with the load. When the source-load connection, it is therefore essential to take into account the variable nature of the power issued by the PV generator but also characteristic of the load to a point of operation is possible. The operating point corresponds to the intersection of these two characteristics (Fig. 9).

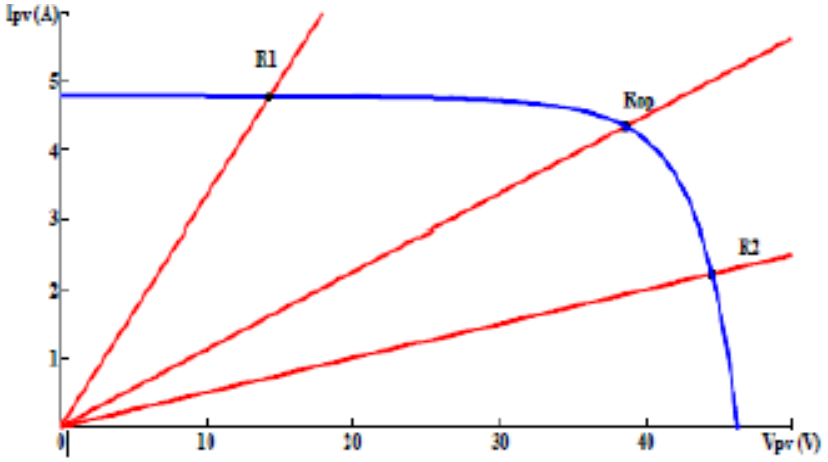

Fig. 9: Influence of the load on the operating point

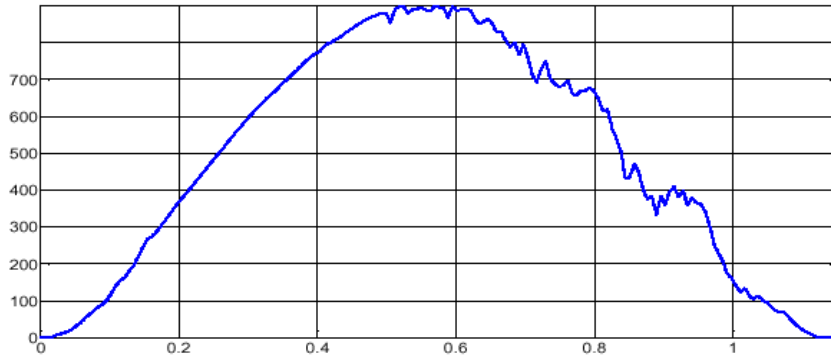

Fig. 10: Variation of the light during a day

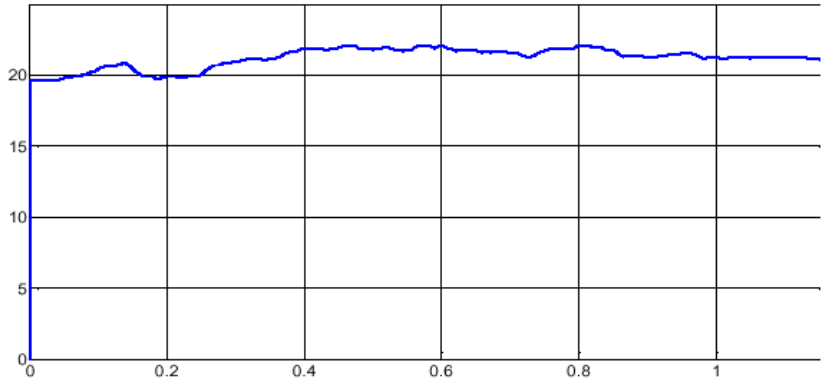

Fig. 11: Variation of the temperature during a day

The operation of the generator is highly dependent on characteristics of the load with which it is connected. In addition, for different values of R, adaptation optimal product for a single operating point of (R_{op}) called expired maximum power point (maximum point power) MPP. Accordingly, so that the generator operates the most often at its maximum point, the solution commonly used is to introduce a converter DC/DC playing the role of load source adapter in this case, the generator delivers a maximum power. Indeed, renewable energy is an important subject of research in the field of industry. The research center has been UDES acquisition of several weather data the 2 years 2012-2013. Among these data, the temperature and light radiation. In this present work, the day chosen is 04 June 2012. Figure 10 and 11 show the variation solar radiation and the temperature variation during the

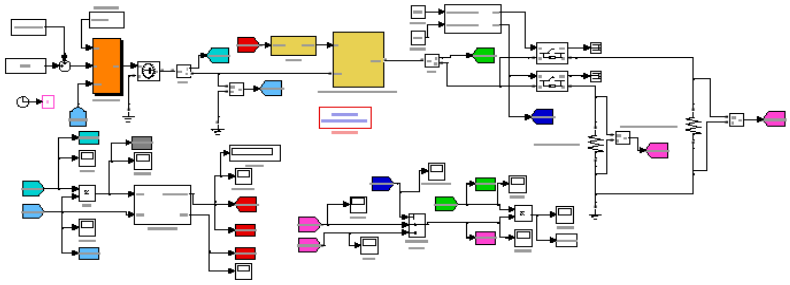

Fig. 12: The proposed system for controlled power of a photovoltaic panel

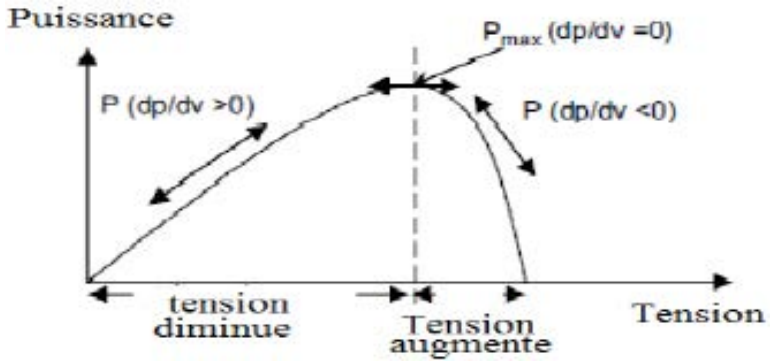

Fig. 13: Characteristic of the PV generator power

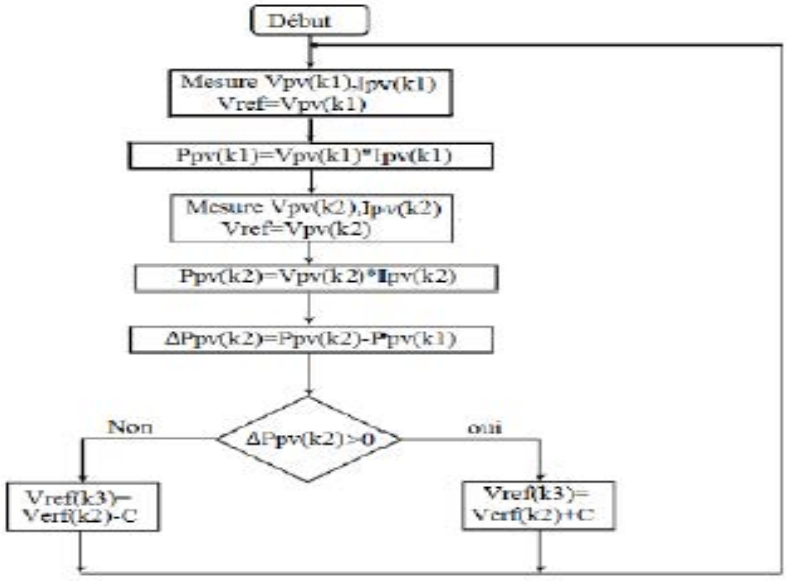

Fig. 14: Algorithm Disturbance and Observation (P and O)

day. Normalization of the done. A consumption control system of the power of photovoltaic panel is shown in Fig. 12. This system is composed mainly from a photovoltaic generator GPV, a DC-DC converter based on a parallel boost chopper (BOOST), a load variable resistive and Blur regulator.

Disturbance and control observation (p and o): The principle of this command is to generate disturbances by reducing or increasing the ratio cyclic D and observe the effect on the power delivered by GPV (Fig. 13). The algorithm of this command is shown in Fig. 14. If dpv/dVpv >0, the voltage is increased, this induces an

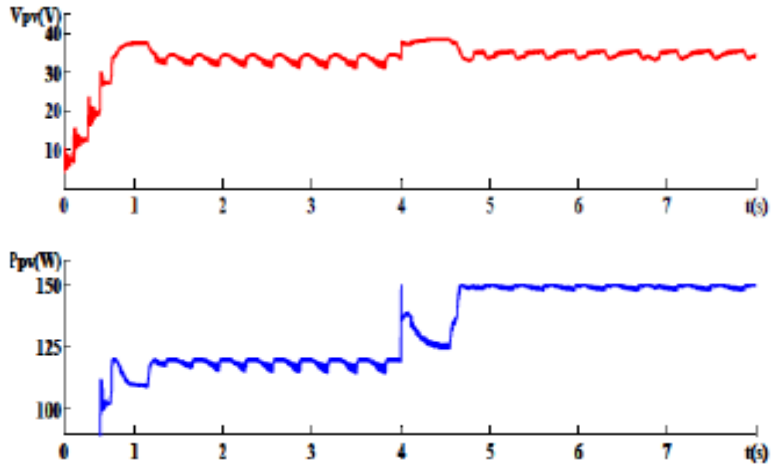

Fig. 15: Allure of the voltage and power face a variation of brightness

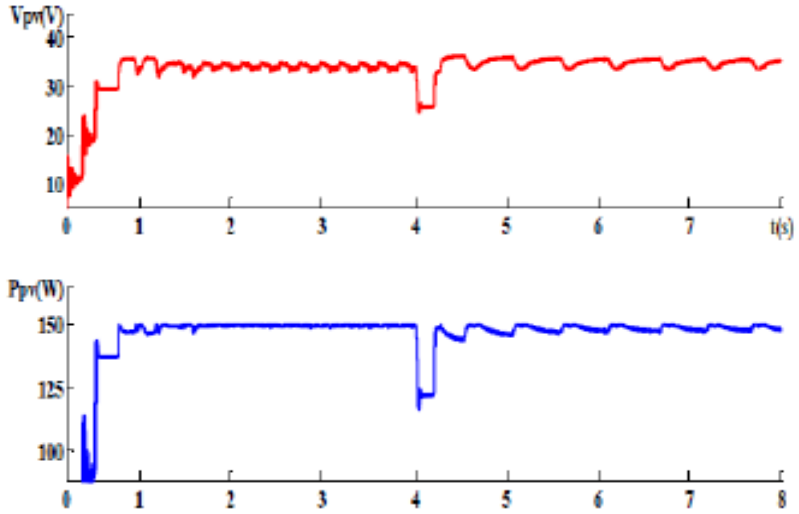

Fig. 16: Shape of voltage and power against a variation in load

increase in the duty ratio D (k) = D (k-1)+C. C is a constant of incrementing. If dpv/dVpv<0, the voltage is reduced it this translated by reducing the cyclic ratio D (k) = D (k-1)-C. The results of the simulation of the PV system using the perturbation algorithm and observation (P and O) are shown in Fig. 15 and 16. Initially, we submitted to the system a brightness variation from 800-1000 W/m^2 at the instant t = 4 sec. Therefore, we find in Fig. 15, a increasing the voltage that induces a decrease in the power, the operating point of the system departs MPP after 0.7s. The order dates back point operation is stabilized at the turn of the MPP with certain oscillation which is caused by the algorithm command.

RESULTS AND DISCUSSION

Secondly to verify the behavior of the system to a variation in load we increase it from 10-15 Ω and we keep constant brightness (1000 W/m^2) at time t = 4 sec, the results of the simulation are shown in Fig. 16. The increase in load causes the decrease of the voltage and power (Fig. 16), the point of operation (MPP) moves away and moves in the part left of the power characteristic (Fig. 13). After 0.2 sec the system converges to MPP despite the presence of the disruption.

Order MPPT fuzzy logic: Recently, the fuzzy logic control was used in the maximum point tracking systems MPPT power, this control offers the advantage of being a robust and relatively simple to develop and control it does not require knowledge of the exact model

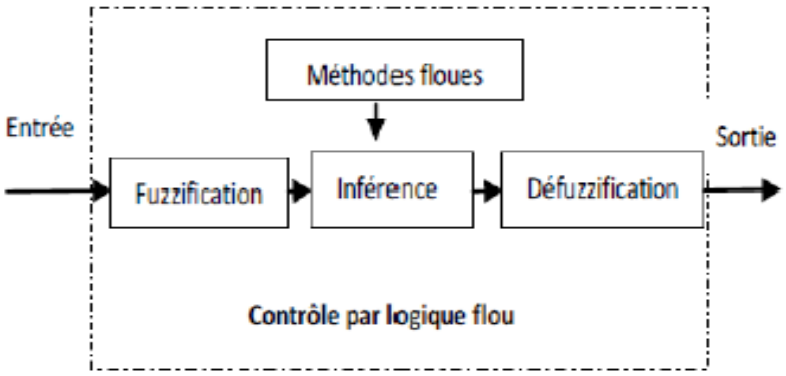

Fig. 17: Principle of fuzzy logic control

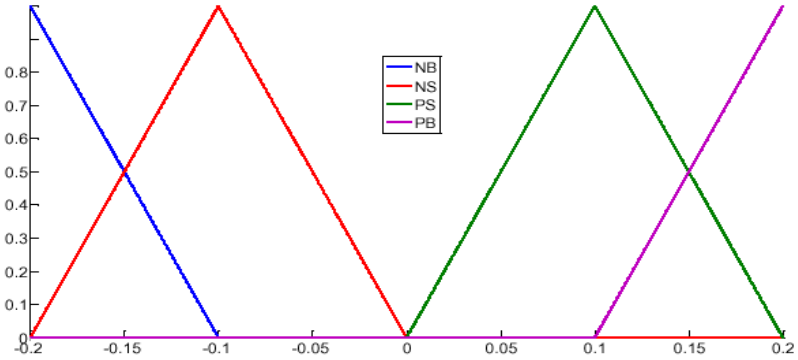

Fig. 18: The membership functions of the power variation ΔP

regulate. The establishment of a fuzzy controller is realized by three stages which are: fuzzification, inference and defuzzification (Fig. 17). The fuzzification helps make the variables blur input. A preliminary step is to define a maximum range of variation allowed for the variables entries. The purpose of the fuzzification is to transform input variables into linguistic variables or variable blurred. In our case, there are two input variables which are the error E (k) and CE (k) error variation at time k that are defined as follows:

$$E(k) = [P_{pv}(k)-P_{pv}(k-1)]/[V_{pv}(k)-V_{pv}(k-1)] \quad (23)$$

$$CE(k) = E(k)-E(k-1) \quad (24)$$

Inference is a step of defining a logical relationship between inputs and output. Indeed, membership rules will be set for the exit as it was done for the inputs, thanks to these rules. Obviously, a good knowledge of the system is required for the development of such a regulator. Indeed in general, an input value is defined by two fuzzy functions with different degrees and the output will also be defined by several functions. The question is to know what degrees of belonging. Several methods can answer this question. From our part, we used the MAX-MIN method. Finally, we must realize the inverse of fuzzification, here we have to calculate a numeric value understandable to the outside environment from a vague definition is what is the aim of defuzzification. Indeed, the fuzzy controller objective is to find the MPPT point of the photovoltaic panel. This works on a fuzzy algorithm has two .DELTA.V and .DELTA.P inputs and one output which is a step ΔVref variable to increase or decrease the reference voltage Vref. This variation is given by the following equation:

$$V_{ref}(K) = V_{ref}(k-1)+\Delta V_{ref} \quad (25)$$

The memberships of these input/output functions are shown in Fig. 18-20, respectively. The fuzzy controller based on fuzzy logic type 1 with triangular membership functions. This method develops modified P and O (Fig. 21). The method applied is min-max functions of previous affiliations. Calculating Δv_{ref} is performed from the center of gravity method is represented by the following expression:

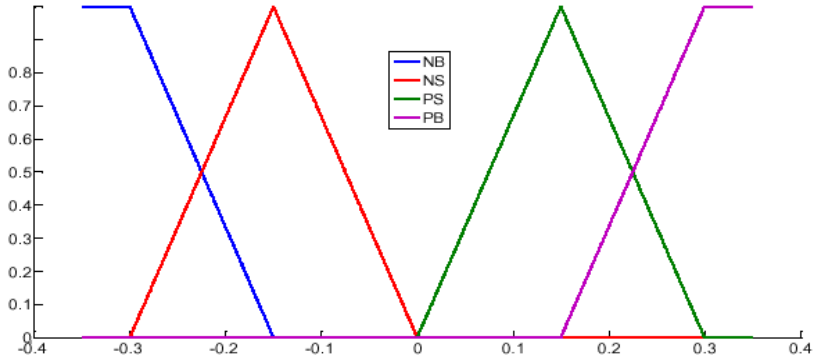

Fig. 19: The membership functions for the variation of the voltage ΔV

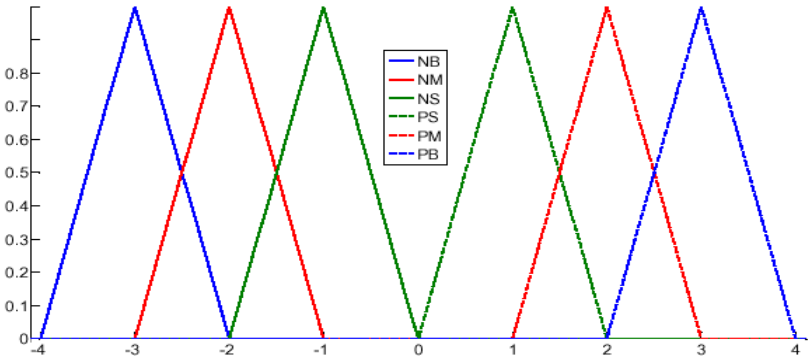

Fig. 20: The duties of membership of the output ΔV_{ref}

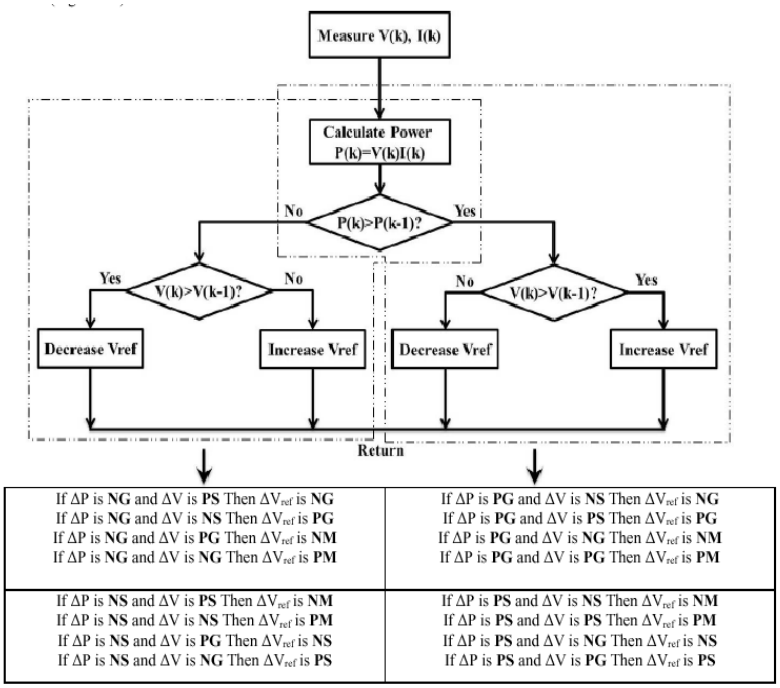

If ΔP is **NG** and ΔV is **PS** Then ΔV_{ref} is **NG** If ΔP is **NG** and ΔV is **NS** Then ΔV_{ref} is **PG** If ΔP is **NG** and ΔV is **PG** Then ΔV_{ref} is **NM** If ΔP is **NG** and ΔV is **NG** Then ΔV_{ref} is **PM**	If ΔP is **PG** and ΔV is **NS** Then ΔV_{ref} is **NG** If ΔP is **PG** and ΔV is **PS** Then ΔV_{ref} is **PG** If ΔP is **PG** and ΔV is **NG** Then ΔV_{ref} is **NM** If ΔP is **PG** and ΔV is **PG** Then ΔV_{ref} is **PM**
If ΔP is **NS** and ΔV is **PS** Then ΔV_{ref} is **NM** If ΔP is **NS** and ΔV is **NS** Then ΔV_{ref} is **PM** If ΔP is **NS** and ΔV is **PG** Then ΔV_{ref} is **NS** If ΔP is **NS** and ΔV is **NG** Then ΔV_{ref} is **PS**	If ΔP is **PS** and ΔV is **NS** Then ΔV_{ref} is **NM** If ΔP is **PS** and ΔV is **PS** Then ΔV_{ref} is **PM** If ΔP is **PS** and ΔV is **NG** Then ΔV_{ref} is **NS** If ΔP is **PS** and ΔV is **PG** Then ΔV_{ref} is **PS**

Fig. 21: Fuzzification rules of P and O method

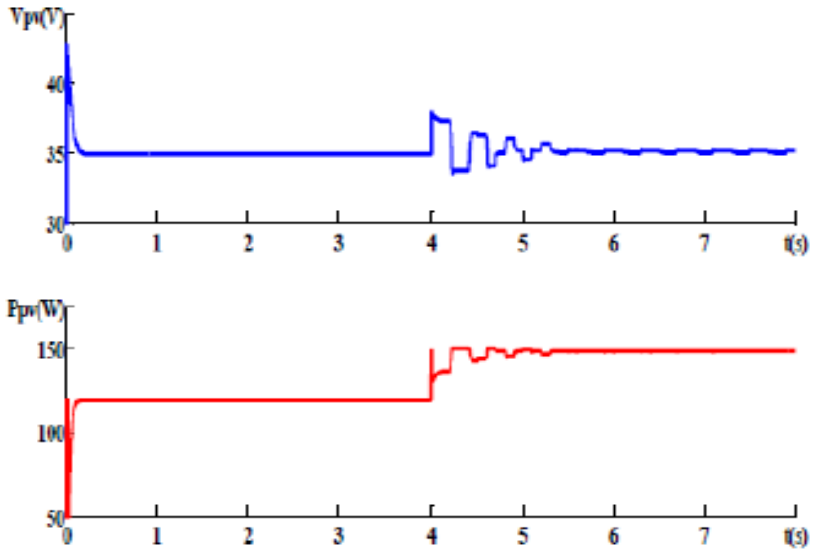

Fig. 22: Shape of voltage and power front a variation of brightness

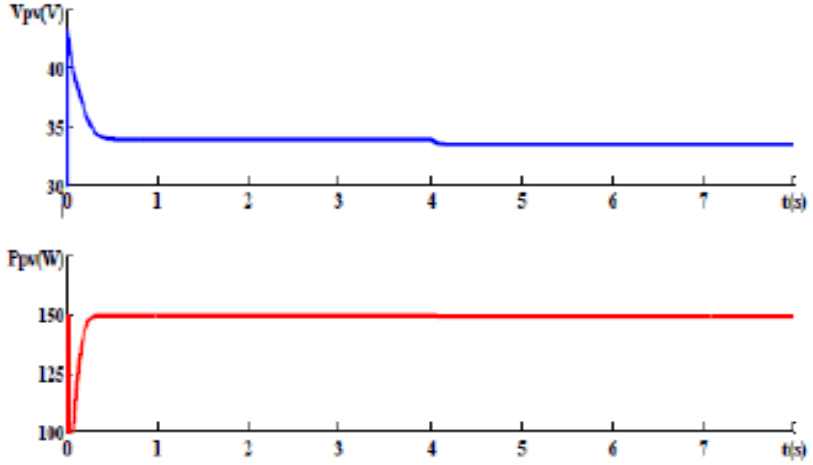

Fig. 23: Shape of voltage and power front to a variation in load

$$\Delta_{ref} = \frac{\sum_i^n \Delta V_{refi}\, \mu(\Delta V_{refi})}{\sum_i^n \mu(\Delta V_{refi})} \quad (26)$$

After simulation of the system with MPPT control blurred for the same dimming conditions and load applied to previous orders. Figure 22 and 23 show the results of simulation fuzzy MPPT system. In the case of a disturbance caused by the change in brightness, the system converges to MPP and remains stable with a small ripple rate compared to other types of control but with a convergence time most important of around 1.3 s (Fig. 22). However, when a disturbance due to the load, the system is insensitive disturbance, power remains stable and does not undergo significant fluctuations (Fig. 23).

A nother result can be studied like In this simulation, a sudden change is applied at the resistive load. An abrupt change is made at time t = 0.5 a 200 Ω resistance 20 Ω and another change is made at time t = 0.8 resistance of 20-200 Ω as shown in Fig. 24. A sudden change of 200 Ω load resistance 20 Ω at time 0.5-200 and 20 Ω at time 0.8. The fuzzy algorithm shows better performance at the search level MPPT issue. A better continue at the current, voltage and power as shown in Fig. 25-28. Figure 26 shows the change in the no ΔVref to catch and correct the change made at the current level due to the sudden change in load.

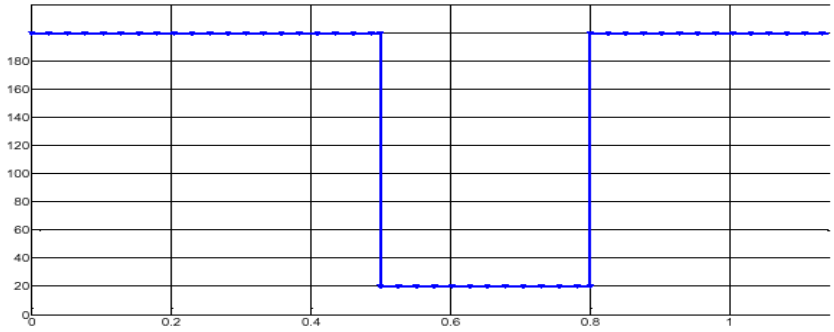

Fig. 24: Sudden change is applied at the resistive load

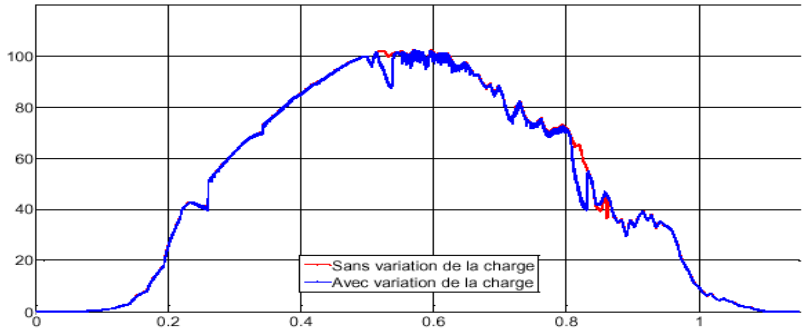

Fig. 25: The variation of the power with and without the change in the load

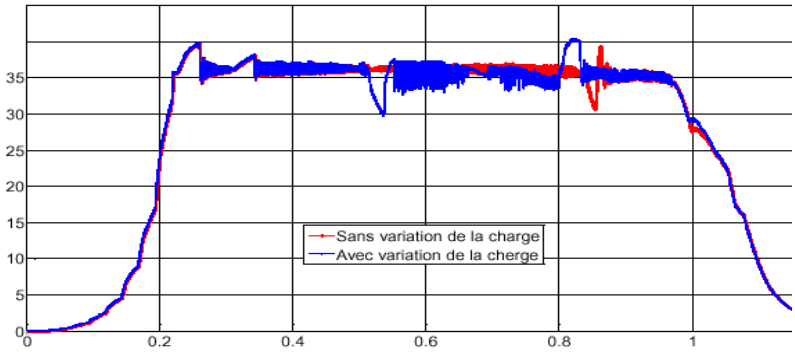

Fig. 26: The current variation with and without the change in load

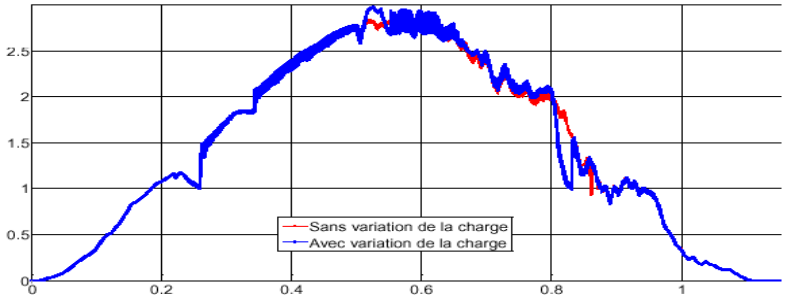

Fig. 27: The variation of the voltage with and without the change in load

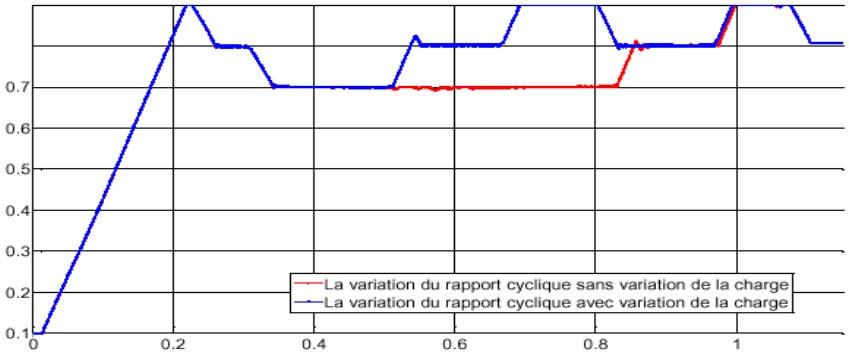

Fig. 28: The pitch variation of the reference voltage with and without the change in the load

CONCLUSION

The main objective of this work is to study and propose a system which is modeled and simulated on MATLAB using Simulink and SimPower Systems (SPS) set Toolboxes. The performance of the proposed system is presented to demonstrate its capability of MPPT, harmonic elimination, load balancing and load leveling. For MPPT Model, despite excellent performances which begin with dynamic response of the system, the results are satisfactory and interesting that is not guaranteed beyond 300 stations. Thus the main objective is to integrate the Renewable Energy Sources (RES) and the utility grid with the electrical load of NZEB. Using wind turbine parameters.

REFERENCES

Bose, B.K., P.M. Szczeny and R.L. Steigerwald, 1985. Microcomputer control of a residential photovoltaic power conditioning system. IEEE Trans. Ind. Electron., IA-21: 1182-1191.

Campbell, R.C., 2007. A circuit-based photovoltaic array model for power system studies. Proceedings of the 39th North American Power Symposium, September 30-October 2, 2007, Las Cruces, NM., USA., pp: 97-101.

Celik, A.N., 2003. Long-term energy output estimation for photovoltaic energy systems using synthetic solar irradiation data. Energy, 28: 479-493.

Chiang, S.J., K.T. Chang and C.Y. Yen, 1998. Residential photovoltaic energy storage system. IEEE Trans. Ind. Electron., 45: 385-394.

Chim, C.S., P. Neelakantan, H.P. Yoong and K.T.K. Teo, 2011. Fuzzy logic based MPPT for photovoltaic modules influenced by solar irradiation and cell temperature. Proceedings of the 13th International Conference on Computer Modelling and Simulation, March 30-April 1, 2011, Cambridge, UK., pp: 376-381.

DenHerder, T., 2006. Design and simulation of photovoltaic super system using simulink. Ph.D. Thesis, California Polytechnic State University, San Luis Obispo, CA., USA.

Dondi, D., A. Bertacchini, D. Brunelli, L. Larcher and L. Benini, 2008. Modeling and optimization of a solar energy harvester system for self-powered wireless sensor networks. IEEE Trans. Ind. Electron., 55: 2759-2766.

Khouzam, K.Y., 1990. Optimum load matching in direct-coupled photovoltaic power systems-application to resistive loads. IEEE Trans. Energy Convers., 5: 265-271.

Luque, A. and S. Hegedus, 2003. Handbook of Photovoltaic Science and Engineering. 1st Edn., John Wiley and Sons, England.

Maheshappa, H.D., J. Nagaraju and M.V.K. Murthy, 1998. An improved maximum power point tracker using a step-up converter with current locked loop. Renew. Energy, 13: 195-201.

Moller, H.J., 1993. Semiconductors for Solar Cells. Artech House Inc., Boston, MA., USA., ISBN-13: 978-0890065747, Pages: 343.

Muljadi, E., 1997. PV water pumping with a peak-power tracker using a simple six-step square-wave inverter. IEEE Trans. Ind. Appl., 33: 714-721.

Protin, L. and S. Astier, 1997. Convertisseurs photovoltaiques. Technique de l'Ingenieur. http://www.thierry-lequeu.fr/data/PAP622.HTM.

Taha, M.S. and K. Suresh, 1996. Maximum power point tracking inverter for photovoltaic source pumping applications. Proceedings of the International Conference on Power Electronics, Drives and Energy Systems for Industrial Growth, Volume 2, January 8-11, 1996, New Delhi, India, pp: 883-886.

Tsuda, I., K. Kurokawa and K. Nozaki, 1994. Annual simulation results of PV system with redox flow battery. Solar Energy Mater. Solar Cells, 35: 503-508.